Vol 16 No 4, April 2007
1009-1963/2007/16(04)/1062-10
Chinese Physics
© 2007 Chin. Phys. Soc.
and IOP Publishing Ltd

Mechanism of the excitation of single pure mode $L(0,2)$ and its interaction with the defect in a hollow cylinder*

Tang Li-Guo(汤立国)[a)b)†], Cheng Jian-Chun(程建春)[c)‡], and Xu Xiao-Mei(许肖梅)[a)b)]

[a)] *Department of Oceanography, Xiamen University, Xiamen* 361005, *China*
[b)] *Key Laboratory of Underwater Acoustic Communication and Marine Information Technology, Ministry of Education, Xiamen University, Xiamen* 361005, *China*
[c)] *Laboratory of Modern Acoustics and Institute of Acoustics, Nanjing University, Nanjing* 210093, *China*

(Received 13 September 2006; revised manuscript received 7 November 2006)

Guided elastic waves have a great potential in pipe inspection as an efficient and low-cost nondestructive evaluation (NDE) technique, among which the wave of mode $L(0,2)$ receives a lot of attention because this mode is the fastest mode in a weakly dispersive region of frequency to minimize dispersion effects over a long distance and sensitive to the defects distributed circumferentially. Though many experimental and numerical researches have already been carried out about the excitation of $L(0,2)$ and its interaction with the defect in a hollow cylinder, its excitation mechanism has not been clarified yet. In this paper based on the transient response solution of the hollow cylinder, derived by the method of eigenfunction expansion, the theory about the exciting mechanism of mode $L(0,2)$ is advanced and the effects of the spatial distribution, vibration frequency and direction of the external force on the excitation are discussed. And the pure mode $L(0,2)$ is excited successfully under the parameters obtained through theoretical analysis. Furthermore, its interactions with some kinds of defects in hollow cylinders are simulated with the method of finite element analysis (FEA) and the results agree well with those obtained by other researchers.

Keywords: excitation, $L(0,2)$ mode, hollow cylinder, eigenfunction expansion
PACC: 4320, 6230

1. Introduction

Thousands of miles of pipelines are used in oil, chemical, power generating and other industries. In order to inspect them regularly, those industries cry for nondestructive evaluation (NDE) techniques that have not only a high efficiency but also a low cost. Ultrasonic guided waves have a great potential to be used as an NDE technique because they can inspect an area simultaneously without detaching all the insulations from the outer wall of pipe. There are numerous axisymmetric and non-axisymmetric guided wave modes propagating in a hollow cylinder and their application in NDE has been studied for decades.[1−11] It is difficult to analyse the waves reflected from the defects if the incident wave has multiple modes. So it is important to study how to excite some single pure mode and use it to detect the defects in hollow cylinders. Lowe *et al*[4−7] have suggested the usage of the $L(0,2)$ mode, which is the fastest mode in a weakly dispersive region of frequency to minimize dispersion effects over a long distance and sensitive to the defects distributed circumferentially. Though the method of generating the $L(0,2)$ mode and its interaction with defects have been studied in many papers,[4−8] its excitation mechanism has not yet been explained clearly. The main aim of this paper is to enunciate the mechanism of the excitation of mode $L(0,2)$ and the influences of the spatial distribution, vibration frequency and direction of the external force on the excitation based on the transient response solution of a hollow cylinder, derived by the method of eigenfunction expansion which is important for solving elastodynamic problems.[12−16] Furthermore, the interactions of mode $L(0,2)$ with different kinds of defects in hollow cylinders have been simulated with the method of finite element analysis (FEA).

*Project supported by the Research Startup Fund for New Research Staff of Xiamen University, China.
†E-mail: liguotang@xmu.edu.cn
‡E-mail: jccheng@nju.edu.cn

2. Method of eigenfunction expansion

The motion of an isotropic homogeneous elastic body with an externally applied force density $\boldsymbol{f}(\boldsymbol{r},t)$ in the body V and a force density $\boldsymbol{s}(\boldsymbol{r},t)$ at the surface Σ, respectively, is governed by elastodynamic equation

$$\begin{aligned}\boldsymbol{L}(\boldsymbol{u}) \equiv (\lambda+\mu)\nabla(\nabla\cdot\boldsymbol{u})+\mu\nabla^2\boldsymbol{u}\\ =\rho\frac{\partial^2\boldsymbol{u}}{\partial t^2}-\rho\boldsymbol{f}(\boldsymbol{r},t),\quad \boldsymbol{r}\in V,\end{aligned}\tag{1}$$

with the boundary condition

$$\begin{aligned}\boldsymbol{B}(\boldsymbol{u}) \equiv (\lambda(\nabla\boldsymbol{u})+\mu[\nabla\boldsymbol{u}+(\nabla\boldsymbol{u})^t])\cdot\boldsymbol{n}\\ =\boldsymbol{s}(\boldsymbol{r},t),\quad \boldsymbol{r}\in\Sigma\,,\end{aligned}\tag{2}$$

where λ and μ are the Lamé constants of the material, and $\boldsymbol{u}(\boldsymbol{r},t)$ is the displacement field vector.

If the elastic body is a hollow cylinder as shown in Fig.1, the eigenvalue problem of the linear differential operator $\boldsymbol{L}$ is determined by

$$\boldsymbol{L}[\boldsymbol{u}_{nmk}]=-\rho\omega_{nmk}^2\boldsymbol{u}_{nmk},\quad (\boldsymbol{r}\in V),\tag{3}$$

$$\boldsymbol{B}[\boldsymbol{u}_{nmk}]=0,\quad (\boldsymbol{r}\in\Sigma)\,.\tag{4}$$

Note that Eq.(4) implies that the boundary conditions of inner and outer lateral surfaces of the hollow cylinder are traction-free while those of two end surfaces of it are rigid-smooth. It has been shown that the eigenvalues are real and nonnegative.[12] Furthermore, the linear differential operator $\boldsymbol{L}$ is self-adjoint under the boundary operator $\boldsymbol{B}$.[13,14] Therefore the eigenmodes $\{\boldsymbol{u}_{nmk}\}$ form an orthogonal set, that is,

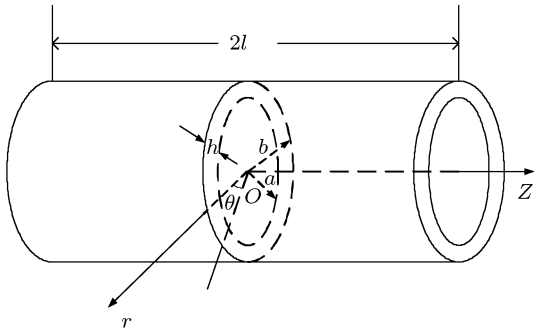


Fig.1. A hollow cylinder with length $2l$, outer radius b and wall thickness h.

$$\int_V\rho\,\boldsymbol{u}_{nmk}\cdot\boldsymbol{u}_{pqj}\mathrm{d}V=\begin{cases}0, & n\neq p \text{ or } m\neq q \text{ or } k\neq j,\\ M_{nmk}, & n=p,\ m=q \text{ and } k=j,\end{cases}\tag{5}$$

where M_{nmk} is the norm of $\boldsymbol{u}_{nmk}$

$$M_{nmk}=\int_{-l}^{l}\int_0^{2\pi}\int_a^b\rho\boldsymbol{u}_{nmk}(r,\theta,z)\cdot\boldsymbol{u}_{nmk}(r,\theta,z)r\mathrm{d}r\mathrm{d}\theta\mathrm{d}z\,.\tag{6}$$

Hence the solution of nonhomogeneous equation (1) can be expanded into

$$\boldsymbol{u}(r,\theta,z,t)=\sum_{nmk}q_{nmk}(t)\mathbf{u}_{nmk}(r,\theta,z),\tag{7}$$

where

$$q_{nmk}(t)=\frac{1}{M_{nmk}\omega_{nmk}}\int_0^t\Phi_{nmk}(\tau)\cdot\sin\omega_{nmk}(t-\tau)\mathrm{d}\tau,\tag{8}$$

$$\Phi_{nmk}(t)=\int_V\boldsymbol{f}(\boldsymbol{r},t)\cdot\boldsymbol{u}_{nmk}(\boldsymbol{r})\mathrm{d}V+\int_\Sigma\boldsymbol{s}(\boldsymbol{r},t)\cdot\boldsymbol{u}_{nmk}(\boldsymbol{r})\mathrm{d}S\,.\tag{9}$$

3. Transient responses of an infinite-length hollow cylinder

Equations (7)–(9) are the transient responses of a finite-length hollow cylinder while the densities of body and surface forces applied to it are $\boldsymbol{f}(\boldsymbol{r},t)$ and $\boldsymbol{s}(\boldsymbol{r},t)$ respectively. As the hollow cylinder is infinite in length, that is, $l\to\infty$, the interval between two successive wave numbers $\Delta\xi_k=\pi/l$ approaches zero, which means that the variable ξ is continuous, not dis-

crete. Therefore in the limit of l approaching infinity, the summation over the index k in Eq.(7) will be replaced by the integral over the continuous eigenvalue ξ. Then we have

$$\boldsymbol{u}(r,\theta,z,t)=\int_0^\infty \mathrm{d}\xi \sum_{nm} q_{nm}(t)\boldsymbol{u}_{nm}(r,\theta,z), \tag{10}$$

where

$$q_{nm}(t)=\frac{1}{M_{nm}\omega_{nm}}\int_0^t \Phi_{nm}(\tau) \cdot \sin\omega_{nm}(t-\tau)\mathrm{d}\tau, \tag{11}$$

$$\Phi_{nm}(t)=\int_V \boldsymbol{f}(\boldsymbol{r},t)\cdot\boldsymbol{u}_{nm}(\boldsymbol{r})\mathrm{d}V + \int_\Sigma \boldsymbol{s}(\boldsymbol{r},t)\cdot\boldsymbol{u}_{nm}(\boldsymbol{r})\mathrm{d}S. \tag{12}$$

If an external force which is symmetrical with respect to $z=0$ is applied to the outer surface of the hollow cylinder radially, we will have

$$\boldsymbol{f}(\boldsymbol{r},t)=0 \tag{13}$$

and

$$\boldsymbol{s}(\boldsymbol{r},t)=b^{-1}f(\theta)g(z)T(t)\boldsymbol{e}_r. \tag{14}$$

Substituting Eqs.(13) and (14) into Eqs.(10)–(12), we obtain

$$\boldsymbol{u}(r,\theta,z,t)=\int_0^\infty \mathrm{d}\xi \sum_{nm}\Big[\frac{R^r_{nm}(b,\xi,\omega_{nm})}{M_{nm}\omega_{nm}}\cdot\varepsilon_1\cdot\varepsilon_2 \cdot\int_0^t T(\tau)\cdot\sin\omega_{nm}(t-\tau)\mathrm{d}\tau\Big] \cdot\boldsymbol{u}_{nm}(r,\theta,z), \tag{15}$$

where

$$\boldsymbol{u}_{nm}(r,\theta,z)=u^r_{nm}(r,\theta,z)\boldsymbol{e}_r+u^\theta_{nm}(r,\theta,z)\boldsymbol{e}_\theta + u^z_{nm}(r,\theta,z)\boldsymbol{e}_z, \tag{16}$$

$$u^r_{nm}(r,\theta,z)=R^r_{nm}(r,\xi,\omega_{nm})\cos n\theta\cos\xi z, \tag{17}$$

$$u^\theta_{nm}(r,\theta,z)=R^\theta_{nm}(r,\xi,\omega_{nm})\sin n\theta\cos\xi z, \tag{18}$$

$$u^z_{nm}(r,\theta,z)=R^z_{nm}(r,\xi,\omega_{nm})\cos n\theta\sin\xi z\,, \tag{19}$$

and

$$\varepsilon_1=\int_0^{2\pi} f(\theta)\cos n\theta\mathrm{d}\theta\,, \tag{20}$$

$$\varepsilon_2=\int_{-L}^{L} g(z)\cos\xi z\mathrm{d}z\,. \tag{21}$$

if the surface forces are axisymmetric. Similarly, if the external force which is antisymmetrical with respect to $z=0$ is applied to the outer surface of the hollow cylinder axially and axisymmetrically, we will have Eq.(13) and

$$\boldsymbol{s}(\boldsymbol{r},t)=b^{-1}f(\theta)g(z)T(t)\boldsymbol{e}_z\,. \tag{22}$$

Substituting Eqs.(13) and (22) to Eqs.(10)–(12), we have

$$\boldsymbol{u}(r,\theta,z,t)=\int_0^\infty \mathrm{d}\xi \sum_{nm}\Big[\frac{R^z_{nm}(b,\xi,\omega_{nm})}{M_{nm}\omega_{nm}}\cdot\varepsilon_1\cdot\varepsilon_2 \cdot\int_0^t T(\tau)\cdot\sin\omega_{nm}(t-\tau)\mathrm{d}\tau\Big] \cdot\boldsymbol{u}_{nm}(r,\theta,z), \tag{23}$$

where

$$u^r_{nm}(r,\theta,z)=R^r_{nm}(r,\xi,\omega_{nm})\cos n\theta\sin\xi z\,, \tag{24}$$

$$u^\theta_{nm}(r,\theta,z)=R^\theta_{nm}(r,\xi,\omega_{nm})\sin n\theta\sin\xi z\,, \tag{25}$$

$$u^z_{nm}(r,\theta,z)=R^z_{nm}(r,\xi,\omega_{nm})\cos n\theta\cos\xi z\,, \tag{26}$$

$$\varepsilon_2=\int_{-L}^{L} g(z)\cos\xi\, z\mathrm{d}z\,, \tag{27}$$

and ε_1 is determined by Eq.(20).

4. Mechanism of the excitation of single pure mode $L(0,2)$

Figure 2 shows the group velocity dispersive curves of some guided wave modes propagating in the hollow cylinder with outer diameter OD = 88.7 mm, wall thickness $h=5.5$ mm, density

$$\rho=7.8e\times10^3\ \mathrm{kg/m^3},$$

Young's module

$$E=21.504\times10^{10}\ \mathrm{N/m^2}$$

and Poisson coefficient $\gamma=0.28$. These geometrical and material parameters of the hollow cylinder are used in all numerical simulations in this paper. It is easy to find that there are numerous guided wave modes even in a low-frequency region. If multiple modes are excited, the reflected waves from the defects will be too complex to be analysed for useful information about the defects. So it is important to study how to choose and excite some single pure guided wave mode and use it to detect the defects in order to simplify the analysis of the reflected waves. Lowe *et al*[4−7] have suggested the usage of the $L(0,2)$ mode. We can find from Fig.2 that it is the fastest mode in a weakly dispersive region of frequency, which can minimize the dispersion effects over a long distance.

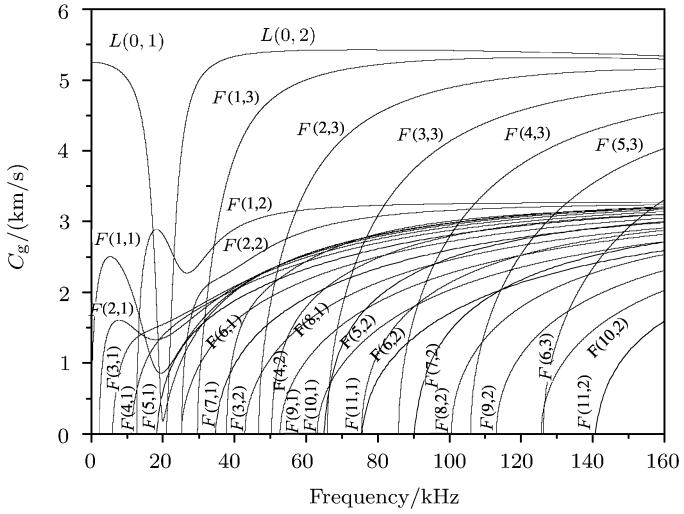


Fig.2. Group velocity dispersive curves for a steel hollow cylinder with OD = 88.7 mm and wall thickness $h = 5.5$ mm.

In order to restrain the excitation of flexural waves, the forces applied to the hollow cylinder should be axisymmetric and run in the full circumference around it. Figure 3 shows a ring of piezoelectric transducer (PZT) surrounding the outer surface of the hollow cylinder. When the PZT vibrates radially or axially, thereby the generated forces are axisymmetric and they can be expressed as Eq.(14) or (22) respectively. And we have

$$f(\theta) = 1, \quad 0 \le \theta < 2\pi, \tag{28}$$

and

$$g(z) = 1, \quad -L \le z \le L. \tag{29}$$

Substituting Eq.(28) to Eq.(20), we have

$$\varepsilon_1 = \begin{cases} 2\pi, & n = 0, \\ 0, & n \neq 0. \end{cases} \tag{30}$$

It is easy to conclude from Eq.(30) that all flexural wave modes have been restrained. At the same time, we can find from Eqs.(18) and (25) that $u^{\theta}_{nm} = 0$ when $n = 0$, which means that torsional wave modes cannot be excited, either. Then we can deduce from Fig.2 that only two modes $L(0,1)$ and $L(0,2)$ can be generated if we restrict the vibrating frequency of PZT in a low-frequency region. It should be noted that the vibrating frequency of PZT must be greater than 60kHz in order to minimize the dispersive effect. And it should be determined according to the geometrical and material parameters of the hollow cylinder. Generally, modes $L(0,2)$ and $L(0,1)$ can be generated simultaneously. So we should take steps to strengthen the excitation of $L(0,2)$ and restrain that of $L(0,1)$. Two steps are adopted to fulfil this aim.

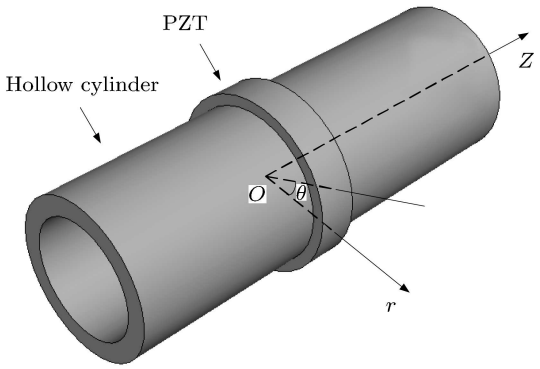


Fig.3. A ring of PZT surrounding the outer surface of a hollow cylinder.

Firstly, we should determine the vibrating direction of the PZT carefully. When the PZT vibrates radially, we can derive from Eq.(15) that

$$\boldsymbol{u}(r,\theta,z,t) = \sum_{m=1}^{2} \left\{ \int_0^{\infty} A_{0m}^{rr} \cdot \cos^2 \xi z \cdot \varepsilon_1 \cdot \varepsilon_2 \cdot \left[\int_0^{t} T(\tau) \cdot \sin \omega_{0m}(t-\tau) \mathrm{d}\tau \right] \mathrm{d}\xi \cdot \boldsymbol{e}_r \right.$$

$$+\int_0^{\infty} A_{0m}^{rz}\cdot\cos\xi z\cdot\sin\xi z\cdot\varepsilon_1\cdot\varepsilon_2\cdot\Big[\int_0^t T(\tau)\cdot\sin\omega_{0m}(t-\tau)\mathrm{d}\tau\Big]\mathrm{d}\xi\cdot\boldsymbol{e}_z\Big\}, \tag{31}$$

where

$$A_{0m}^{rr}(r,\xi,\omega_{0m})=\frac{R_{0m}^{r}(b,\xi,\omega_{0m})\cdot R_{0m}^{r}(r,\xi,\omega_{0m})}{M_{0m}\omega_{0m}},\qquad m=1,2, \tag{32}$$

$$A_{0m}^{rz}(r,\xi,\omega_{0m})=\frac{R_{0m}^{r}(b,\xi,\omega_{0m})\cdot R_{0m}^{z}(r,\xi,\omega_{0m})}{M_{0m}\omega_{0m}},\quad m=1,2\,. \tag{33}$$

Similarly, When the PZT vibrates axially, we can derive from Eq.(23) that

$$\begin{aligned}\boldsymbol{u}(r,\theta,z,t)=\sum_{m=1}^{2}\Big\{&\int_0^{\infty} A_{0m}^{zr}\cdot\sin\xi z\cdot\cos\xi z\cdot\varepsilon_1\cdot\varepsilon_2\cdot\Big[\int_0^t T(\tau)\cdot\sin\omega_{0m}(t-\tau)\mathrm{d}\tau\Big]\mathrm{d}\xi\cdot\boldsymbol{e}_r\\&+\int_0^{\infty} A_{0m}^{zz}\cdot\sin^2\xi z\cdot\varepsilon_1\cdot\varepsilon_2\cdot\Big[\int_0^t T(\tau)\cdot\sin\omega_{0m}(t-\tau)\mathrm{d}\tau\Big]\mathrm{d}\xi\cdot\boldsymbol{e}_z\Big\},\end{aligned} \tag{34}$$

where

$$A_{0m}^{zr}(r,\xi,\omega_{0m})=\frac{R_{0m}^{z}(b,\xi,\omega_{0m})\cdot R_{0m}^{r}(r,\xi,\omega_{0m})}{M_{0m}\omega_{0m}},\quad m=1,2, \tag{35}$$

$$A_{0m}^{zz}(r,\xi,\omega_{0m})=\frac{R_{0m}^{z}(b,\xi,\omega_{0m})\cdot R_{0m}^{z}(r,\xi,\omega_{0m})}{M_{0m}\omega_{0m}},\quad m=1,2. \tag{36}$$

It is reasonable to think that the amplitudes of the axial and radial displacements of $L(0,1)$ and $L(0,2)$ are mainly determined byA_{0m}^{rr}, A_{0m}^{rz}(or A_{0m}^{zr}), A_{0m}^{zz} ($m=1,2$), ε_1 and ε_2 in Eqs.(31) and (34), in which ε_1 and ε_2 reflect the influences of the distributions and sizes of PZTs while the others are determined by the geometrical and material parameters of the hollow cylinder. So we refer to A_{0m}^{rr}, $|A_{0m}^{rz}|$ (or $|A_{0m}^{zr}|$) and A_{0m}^{zz} ($m=1,2$) as the characteristic amplitudes of different displacement components of transient waves $L(0,1)$ and $L(0,2)$. The first letter of the superscript in A_{0m}^{rr} represents the vibrating direction of the PZT while the second letter in it represents the direction of the displacement. The second letter of the subscript in A_{0m}^{rr} represents the order of the wave mode excited. Then A_{0m}^{rr} is the characteristic amplitude of radial displacement of mode $L(0,\ m)$ while the PZT vibrates radially. Figures 4(a), 4(c) and 4(e) show the variations of A_{0m}^{rr}, $|A_{0m}^{rz}|$ (or $|A_{0m}^{zr}|$) and A_{0m}^{zz} ($m=1,2$) with frequency when $r=b$. Figure 4(a) indicates that the characteristic amplitude of radial displacement of $L(0,1)$ is bigger than that of $L(0,2)$ between 40 and 160 kHz when the PZT vibrates radially. The ratio of A_{02}^{rr} to A_{01}^{rr} is given in Fig.4(b), from which we can find the ratio is far less than 1.0 between 50 and 120 kHz. Figure 4(c) shows the characteristic amplitudes of axial displacements of $L(0,1)$ and $L(0,2)$ between 40 and 160 kHz when the PZT vibrates radially or those of their radial displacements while the PZT vibrates axially in the same frequency region. The ratio between them is shown in Fig.4(d). Figures 4(c) and 4(d) indicate that they have no sharp difference on the whole except for in the narrow neighbourhood of 71 kHz. Figure 4(e) indicates that the characteristic amplitude of axial displacement of $L(0,2)$ is much bigger than that of $L(0,1)$ between 40 and 80 kHz when the PZT vibrate axially, which is obvious in Fig.4(f). Our aim is to excite single pure mode $L(0,2)$, that is, the amplitude of $L(0,2)$ excited should be far bigger than that of $L(0,1)$. We are lucky because we can fulfill our aim by making the PZT vibrate axially, which is known from the theoretical analysis above. In a word, the excitation of $L(0,2)$ will be strengthened while that of $L(0,1)$ will be restrained if the PZT vibrates axially in some specific frequency region and the axial displacement component is what is needed.

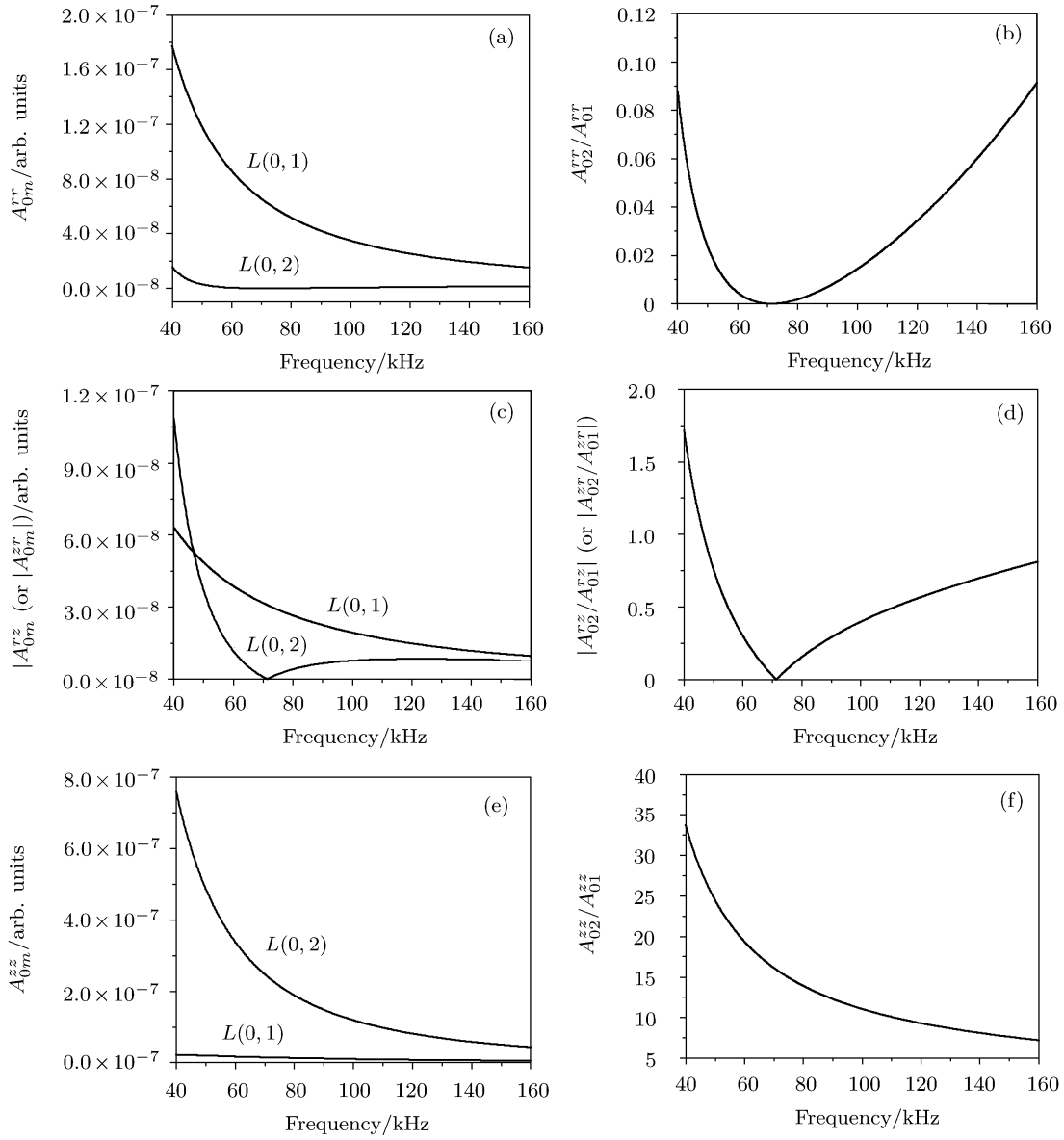


Fig.4. A_{0m}^{rr}, A_{0m}^{rz}(or A_{0m}^{zr}) and A_{0m}^{zz} $(m=1,2)$ in Eqs.(31) and (34) and their ratios as functions of frequency. (a) A_{0m}^{rr}; (b) A_{02}^{rr}/A_{01}^{rr}; (c) $|A_{0m}^{rz}|$ (or $|A_{0m}^{zr}|$); (d) $|A_{02}^{rz}/A_{01}^{rz}|$ (or $|A_{02}^{zr}/A_{01}^{zr}|$); (e) A_{0m}^{zz}; (f) A_{02}^{zz}/A_{01}^{zz}.

In order to strengthen the excitation of $L(0,2)$ and restrain that of $L(0,1)$ further, we adopt two rings of PZTs i.e. PZT A and PZT B as shown in Fig.5. L_{PZT} and L_{S} are the width of each PZT and the central spacing between PZTs respectively, and they should be chosen appropriately. This is just the second step mentioned above. Then we have

$$\begin{aligned} &g(z)=1,\\ &-\frac{L_{\mathrm{S}}+L_{\mathrm{PZT}}}{2}\le z\le -\frac{L_{\mathrm{S}}-L_{\mathrm{PZT}}}{2},\\ &\frac{L_{\mathrm{S}}-L_{\mathrm{PZT}}}{2}\le z\le \frac{L_{\mathrm{S}}+L_{\mathrm{PZT}}}{2}. \end{aligned} \tag{37}$$

Substituting expression (37) into Eq.(27), we have

$$\begin{aligned} \varepsilon_2 = &\int_{-(L_{\mathrm{S}}+L_{\mathrm{PZT}})/2}^{-(L_{\mathrm{S}}-L_{\mathrm{PZT}})/2}\cos\xi z\mathrm{d}z\\ &+\int_{(L_{\mathrm{S}}-L_{\mathrm{PZT}})/2}^{(L_{\mathrm{S}}+L_{\mathrm{PZT}})/2}\cos\xi z\mathrm{d}z, \end{aligned} \tag{38}$$

and therefore

$$\varepsilon_2=\frac{4}{\xi}\cos\frac{\xi L_{\mathrm{S}}}{2}\sin\frac{\xi L_{\mathrm{PZT}}}{2}. \tag{39}$$

When the working frequency of PZTs is known, we can obtain the values of ξ corresponding to each mode through the dispersive equations of guided waves. For example, if the frequency is 100 kHz, the values of ξ

corresponding to $L(0,1)$ and $L(0,2)$ are 314.69 m^{-1} and 114.87 m^{-1} respectively.

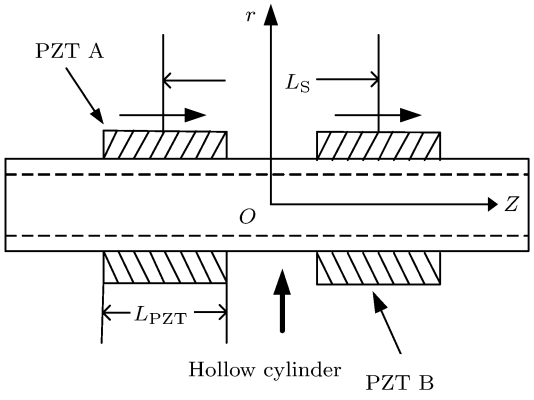


Fig.5. Two rings of PZTs surrounding the outer surface of a hollow cylinder.

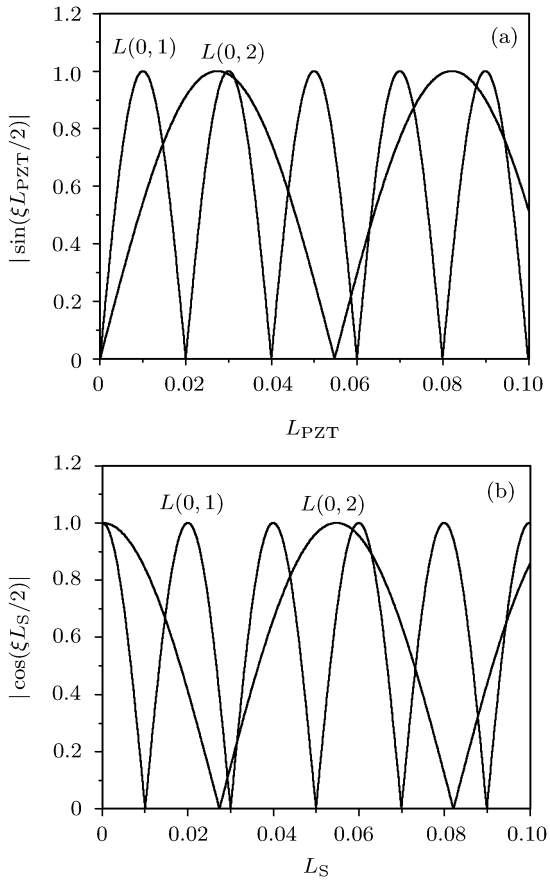


Fig.6. (a) The absolute value of $\sin(\xi L_{PZT}/2)$ as a function of L_{PZT}; (b) The absolute value of $\cos(\xi L_S/2)$ as a function of L_S.

Figure 6(a) shows the relation between $|\sin(\xi L_{PZT}/2)|$ and L_{PZT} while Fig.6(b) shows that between $|\cos(\xi L_S/2)|$ and L_S when the working frequency of PZTs is 100 kHz, i.e. the values of ξ corresponding to modes $L(0,1)$ and $L(0,2)$ are 314.69 m^{-1} and 114.87 m^{-1} respectively. We can find from Figs.6(a) and 6(b) that the excitation of mode $L(0,2)$ can be strengthened while that of mode $L(0,1)$ is well restrained, with the sizes of L_{PZT} and L_S chosen as 2.0 and 5.0 cm respectively.

In conclusion, if we adopt multiple rings of PZTs, appropriately choose the working frequency of PZTs, carefully determine the width of each PZT and spacings between PZTs and make the PZTs vibrate axially, the generated waves will only include modes $L(0,2)$ and $L(0,1)$ and the amplitude of the former will be much greater than that of the latter, i.e. single rather pure mode $L(0,2)$ will be generated. Then it is possible to use the generated wave mode $L(0,2)$ to detect some kinds of defects in the hollow cylinder because the reflected waves are simple enough for analysing the information about the defects.

5. Interaction of mode $L(0,2)$ with the defect in a hollow cylinder

Based on the theory presented above, numerical simulations about the excitation of mode $L(0,2)$ are carried out by the method of FEA. And the interaction of the mode with some kinds of defects in a hollow cylinder is discussed.

5.1. Interactions of mode L(0,2) with full circumferential defects with different depths

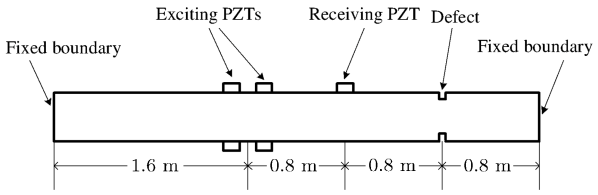


Fig.7. The schematic drawing of exciting and receiving guided waves in a hollow cylinder with a full circumferential defect.

Figure 7 is the schematic drawing of exciting and receiving guided waves. The length of the hollow cylinder is 4.0 m and fixed boundary conditions are adopted at two ends. Two rings of PZTs are used for exciting guided waves and the width of each PZT is 2.0 cm, the central spacing between the two PZTs is 5.0 cm. The distance between the centre of exciting

PZTs and the left end of the hollow cylinder is 1.6 m. The exciting and receiving PZTs are 0.8 m apart. The defect and the right end of the hollow cylinder is 0.8 m apart. The defect is assumed to run in the full circumference around the hollow cylinder and its width is 4.0 mm.

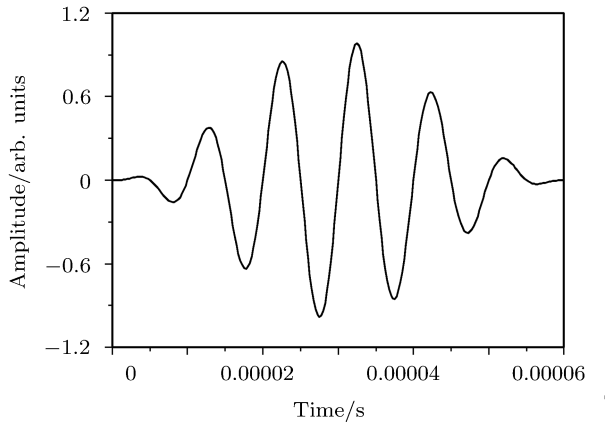


Fig.8. 6 cycles, 100 kHz toneburst modulated by a Hanning window.

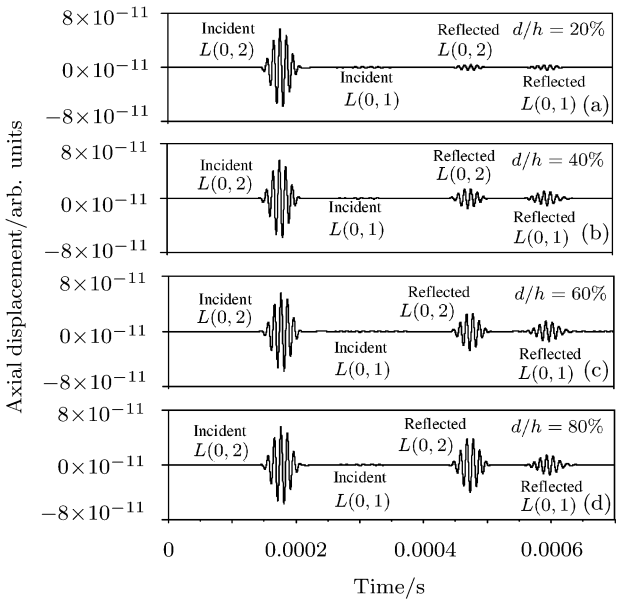


Fig.9. The incident $L(0,2)$ and the reflected waves caused by the interactions of $L(0,2)$ with the defects with different values of d/h. (a) $d/h = 20\%$; (b) $d/h = 40\%$; (c) $d/h = 60\%$; (d) $d/h = 80\%$.

A narrow band signal consisting of 6 cycles, 100 kHz toneburst modulated by a Hanning window is employed as an exciting signal as shown in Fig.8. The exciting PZTs vibrate axially, and the axial displacement is received at the receiving point. Figure 9 shows the incident waves excited and the waves reflected from the defects with different depths. The d and h in the Fig.9 are depth of the defect and wall thickness of the hollow cylinder respectively. We can find from it that not only $L(0,2)$ but also $L(0,1)$ is excited, and the amplitude of $L(0,2)$ is far bigger than that of $L(0,1)$. The reflected waves shown in Fig.9 cannot be caused by the interactions of incident $L(0,1)$ with the defects because the amplitude of reflected wave is bigger than that of incident $L(0,1)$. This can also be verified with the time of receiving the reflected waves. The reflected waves of $L(0,2)$ will arrive before that of $L(0,1)$ because the velocity of $L(0,2)$ is far greater than that of $L(0,1)$.

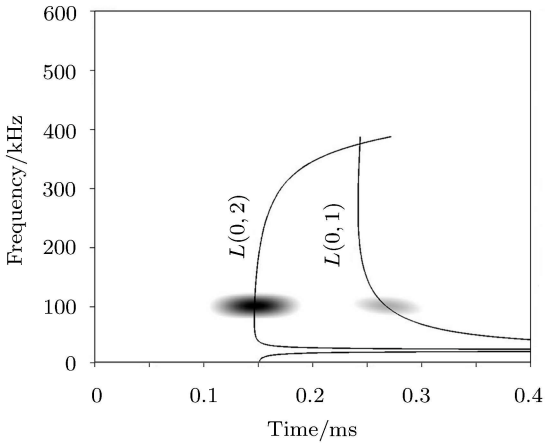


Fig.10. The distributions of time-frequency corresponding to the reflected waves shown in Fig.9(c).

Figure 10 shows the distributions of time-frequency corresponding to the reflected waves shown in Fig.9(c). It clearly shows that the reflected waves are of modes $L(0,2)$ and $L(0,1)$. It should be pointed out that the time for incident $L(0,2)$ to arrive at the defect is the starting time in Fig.10. From the numerical results, we can obtain the reflection coefficients of reflected modes $L(0,2)$ and $L(0,1)$ when the exciting PZTs work at different frequencies as shown in Figs.11(a) and (b). They prove that the higher the frequency, the more sensitive to the defects the guided waves. Figure 11(a) also indicates that the greater the depth, the greater the amplitude of the reflected $L(0,2)$. Figure 11(b) shows that there is a peak value of reflection coefficient of $L(0,1)$. The d/h corresponding to the peak value is denoted with $(d/h)_{\mathrm{p}}$. When the d/h is less than $(d/h)_{\mathrm{p}}$, the greater the depth, the greater the amplitude of the reflected $L(0,1)$. When the d/h is greater than $(d/h)_{\mathrm{p}}$, the greater the depth,

the smaller the amplitude of the reflected $L(0,1)$.

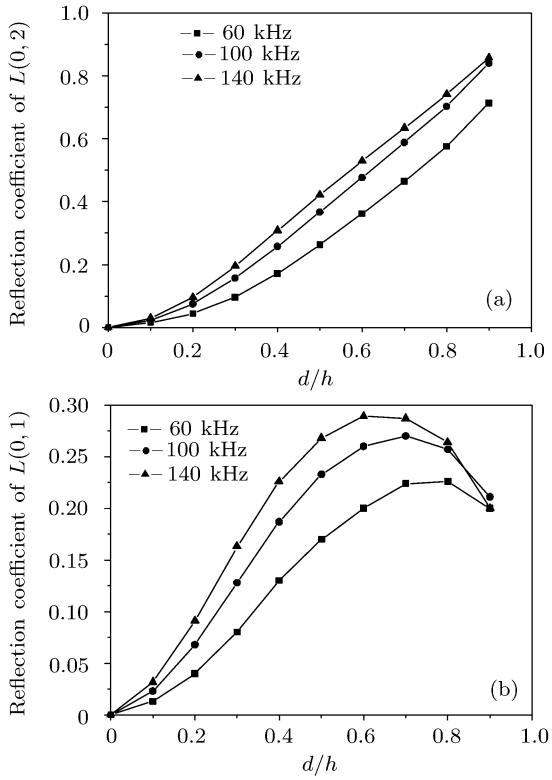


Fig.11. Reflection coefficients of the reflected waves caused by the interaction of $L(0,2)$ with a full circumferential defect in a hollow cylinder as a function of d/h at 60 kHz, 100 kHz and 140 kHz. (a) $L(0,2)$; (b) $L(0,1)$.

5.2. Interactions of mode $L(0,2)$ with the defects with different circumferential lengths

Figure 12 is the schematic drawing of exciting and receiving guided waves in a hollow cylinder with a partial circumferential defect. The length of the hollow cylinder is 10.5m. Symmetrical and fixed boundary conditions are applied to the left and right ends respectively. The length of exciting PZT is 2.32 cm and the distance between the centre of it and the left end of the hollow cylinder is 2.32 cm. The centre of receiving PZT which is located at $\theta = 0$ and the left end of the hollow cylinder are 2.1 m apart. The distance between the defect and the left end of the hollow cylinder is 8.1 m. A narrow band signal consisting of 5 cycles, 80 kHz toneburst modulated by a Hanning window is employed as an exciting signal. Figure 13 shows the incident wave $L(0,2)$ excited. Figure 14 shows the reflected waves caused by the interactions between incident $L(0,2)$ and defects with different circumferential lengths. The $C_{\rm d}$ and $C_{\rm O}$ are outer circumferential length of the defect and the circumference of the hollow cylinder respectively. The widths of all defects are 4.0mm while their depths are half of the wall thickness of the hollow cylinder.

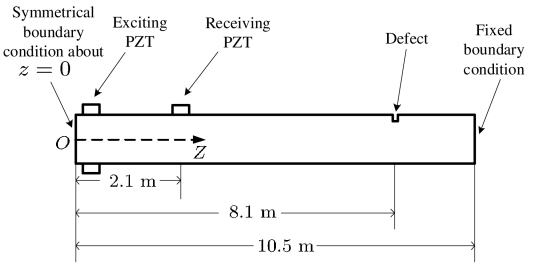


Fig.12. The schematic drawing of exciting and receiving guided waves in a hollow cylinder with a half-thickness and partial circumferential defect.

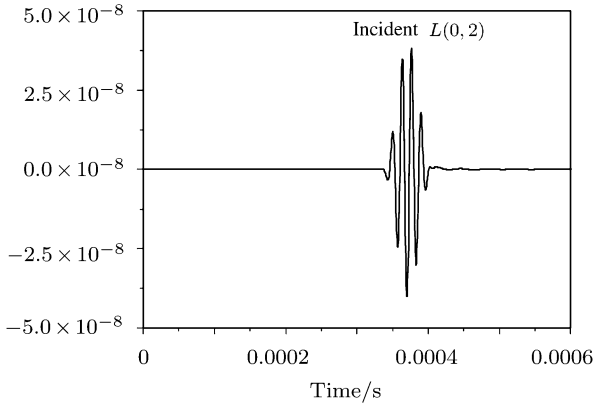


Fig.13. The incident $L(0,2)$ excited.

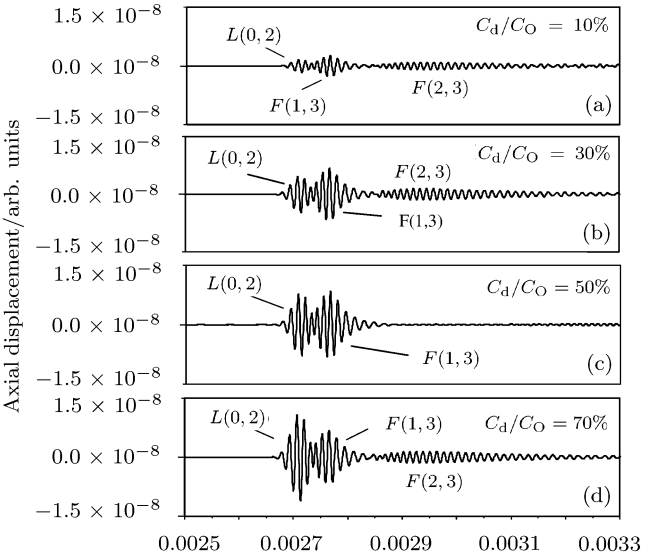


Fig.14. The reflected waves caused by the interactions of incident $L(0,2)$ with the defects with different values of $C_{\rm d}/C_{\rm O}$. (a) $C_{\rm d}/C_{\rm O}$ = 10%; (b) $C_{\rm d}/C_{\rm O}$ = 30%; (c) $C_{\rm d}/C_{\rm O}$ = 50%; (d) $C_{\rm d}/C_{\rm O}$ = 70%.

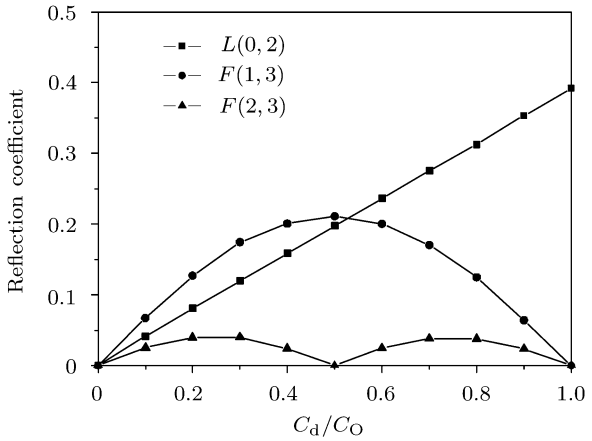


Fig.15. Reflection coefficients of the reflected waves caused by the interaction of $L(0,2)$ with a half-thickness defect in a hollow cylinder at 80 kHz as a function of C_d/C_O.

We can find from Fig.14 that the reflected waves consist of not only axisymmetric mode $L(0,2)$ but also non-axisymmetric modes $F(1,3)$ and $F(2,3)$ during the period of time shown in Fig.14. Mode $L(0,1)$ and some other modes will also be generated in the reflected waves and they will be received later because their velocities are far lower than those of modes $L(0,2)$, $F(1,3)$ and $F(2,3)$. Comparing Fig.14 with Fig.9, we can conclude that the mode conversion occurs after the incident $L(0,2)$ has interacted with the defects and the reflected waves consist of only axisymmetric longitudinal waves if the defects run in the full circumference around the hollow cylinder while they consist of not only axisymmetric longitudinal waves but also non-axisymmetric flexural waves if the defects run in the partial circumference around the hollow cylinder.

From the simulation results as shown in Fig.14, we can obtain the relations of reflection coefficients of modes $L(0,2)$, $F(1,3)$ and $F(2,3)$ with the C_d/C_O as shown in Fig.(15). They are in agreement with the experimental and simulated results obtained by Alleyne *et al.*[4−6] It is clear that the reflection coefficient of $L(0,2)$ is linear with respect to the C_d/C_O while those of modes $F(1,3)$ and $F(2,3)$ are nonlinear.

6. Conclusions

The mechanism of the excitation of mode $L(0,2)$ has been discussed in detail based on the transient response solution of a hollow cylinder, derived by the method of eigenfunction expansion. The excitation of mode $L(0,2)$ is mainly determined by the spatial distributions, sizes, working frequencies and vibrating directions of the PZTs. And the values of these parameters should be chosen according to the geometrical and material parameters of the hollow cylinder. The single pure mode $L(0,2)$ can be excited successfully based on the theory given in this paper. Furthermore, its interactions with some kinds of defects in hollow cylinders have been simulated by the method of FEA. The results agree well with those obtained by other researchers. The procedure of analysing and determining the parameters relating for the PZTs used for exciting mode $L(0,2)$ is also valid for the excitation of some other wave modes.

References

[1] Gazis D C 1959 *J. Acoust. Soc. Am.* **31** 568
[2] Silk M G and Bainton K F 1979 *Ultrasonics* **17** 11
[3] Brook M, Ngoc T D K and Eder J 1990 *Rev. Prog. QNDE* **9** 243
[4] Lowe M J S, Alleyne D N and Cawley P 1998 *Ultrasonics* **36** 147
[5] Alleyne D N, Lowe M J S and Cawley P 1998 *J. Appl. Mech.* **65** 635
[6] Lowe M J S, Alleyne D N and Cawley P 1998 *J. Appl. Mech.* **65** 649
[7] Alleyne D N, Pavlakovic B, Lowe M J S and Cawley P 2001 *Rev. Prog. QNDE* **20** 180
[8] Zhu W H 2002 *J. Pres. Ves. Tech.* **124** 108
[9] Bai H, Shah A H, Popplewell N and Datta S K 2001 *J. Appl. Mech.* **68** 619
[10] Li J and Rose J L 2005 *Ultrasonics* **44** 35
[11] Shin H J and Rose J L 1999 *Ultrasonics* **37** 355
[12] Aringen A C and Suhubi E S 1975 *Elastodynamics* (New York: Academy Press) 438
[13] Weaver R L and Pao Y H 1982 *J. Appl. Mech.* **49** 821
[14] Cheng J C, Zhang S Y and Wu L 1995 *Appl. Phys.* A **61** 311
[15] Qin B, Chen J J and Cheng J C 2005 *Chin. Phys.* **14** 2522
[16] Lu P and Wang Y J 2001 *Acta Phys. Sin.* **50** 697 (in Chinese)